FUEL PROCESSING TECHNOLOGY 89 (2008) 1076–1089

available at www.sciencedirect.com

www.elsevier.com/locate/fuproc

Effect of biomass particle size and air superficial velocity on the gasification process in a downdraft fixed bed gasifier. An experimental and modelling study

Francisco V. Tinaut[a], *Andrés Melgar*[a], *Juan F. Pérez*[b,*], *Alfonso Horrillo*[c]

[a] *Thermal Engines and Renewable Energies Group (MYER), School of Engineering, University of Valladolid, Spain*
[b] *Group of Energy Efficient Management — GIMEL, Engineering Faculty, University of Antioquia, Colombia*
[c] *CIDAUT Research and Development Center in Transport and Energy, Spain*

ARTICLE INFO

Article history:
Received 11 June 2007
Received in revised form
28 April 2008
Accepted 29 April 2008

Keywords:
Biomass
Gasification
Downdraft
Propagation velocity

ABSTRACT

A one-dimensional stationary model of biomass gasification in a fixed bed downdraft gasifier is presented in this paper. The model is based on the mass and energy conservation equations and includes the energy exchange between solid and gaseous phases, and the heat transfer by radiation from the solid particles. Different gasification sub-processes are incorporated: biomass drying, pyrolysis, oxidation of char and volatile matter, chemical reduction of H_2, CO_2 and H_2O by char, and hydrocarbon reforming. The model was validated experimentally in a small-scale gasifier by comparing the experimental temperature fields, biomass burning rates and fuel/air equivalence ratios with predicted results. A good agreement between experimental and estimated results was achieved. The model can be used as a tool to study the influence of process parameters, such as biomass particle mean diameter, air flow velocity, gasifier geometry, composition and inlet temperature of the gasifying agent and biomass type, on the process propagation velocity (flame front velocity) and its efficiency. The maximum efficiency was obtained with the smaller particle size and lower air velocity. It was a consequence of the higher fuel/air ratio in the gasifier and so the production of a gas with a higher calorific value.

1. Introduction

In most cases the gasification of residual biomass without an important level of homogenisation is carried out in fixed bed reactors. According to Hobbs et al. [1], approximately the 89% of the coal gasified in the world has been processed by means of fixed bed technology. Yang et al. [2] concluded that fixed bed gasification or combustion is the most common technology for the energy use of biomass and solid municipal wastes.

During the biomass combustion or gasification process, this renewable material undergoes different sub-processes. In a first step, biomass is dried up. Then, as the temperature increases, biomass is pyrolyzed and the lignin and cellulose are decomposed into volatile molecules such as hydrocarbons, hydrogen, carbon monoxide and water. Finally, the remaining solid fraction, which is called vegetal char, is oxidised when an excess of oxygen is available (combustion). When combustion is developed with less oxygen than the stoichiometric, vegetal char is gasified by the pyrolysis and oxidation gases. This process is governed by the chemical reduction of hydrogen, carbon dioxide and water by char. The inorganic components in the biomass are not volatilised and remain in solid state as ash.

* *Corresponding author*. Tel.: +57 4 219 5550; fax: +57 4 211 0507.
E-mail address: juanpb@udea.edu.co (J.F. Pérez).

0378-3820/$ – see front matter.
doi:10.1016/j.fuproc.2008.04.010

In a significant number of research papers, biomass gasification models of different complexity have been proposed looking for a better understanding of the different subprocesses. Generally, the influence of different parameters on the producer gas composition and its temperature at the exit or along the gasifier is evaluated.

Dimensionless models are useful tools to calculate the final gas composition, assuming that the reactions governing the process are in chemical equilibrium. Ruggiero and Manfrida [3] proposed a model based on chemical equilibrium for studying the effect of different parameters such as biomass elemental composition, equivalence ratio, relative humidity, pressure and temperature, on the gasification process. Other models based on chemical equilibrium are presented in references [4–12].

Yang et al. [13,14] presented a two-dimensional transient model simulating the gasification process of biomass and solid municipal waste in a counter-flow reactor. Within the class of one-dimensional transient models, different approaches have been developed. Shin and Choi [15] and Yang et al. [2,16] took into account the diffusive and species conservation terms in all phases, and the heat transfer by conduction in the solid phase. Di Blasi [17] proposed a model very similar to the previous works, without taking into account the radiative heat transfer along the bed. In another paper, the same author [18] presented similar equations in which the thermal conductivity was taken as a cubic function of temperature coinciding with the usual approach for the heat transfer by radiation. Bruch et al. [19] and Shin and Choi [15] showed that in a packed bed biomass gasifier, the heat transfer by thermal conduction was much lower than the heat transfer by radiation due to the low thermal conductivity of wood.

One-dimensional steady state models of fixed bed downdraft gasifiers have been also proposed. Jayah et al. [20] combined an equilibrium model for the combustion and pyrolysis zone with a one-dimensional steady state model for the char gasification zone (reduction) in order to estimate the temperature profile and species composition along the latter zone as functions of design and process parameters. Giltrap et al. [21] and Babu and Sheth [22] presented a similar model focused on the catalytic effect of char on the heterogeneous reactions in the reduction zone.

Based on the same approach, other authors have modelled updraft gasifiers. Souza–Santos [23] developed a one-dimensional steady state model of the coal gasification/combustion process in a fixed bed counter-flow gasifier. Hobbs et al. [1,24,25] and Ghani et al. [26,27] considered a partial or total equilibrium for the gaseous phase and sub-models for the char devolatilisation. They also adopted the heat transfer by convection in the packed bed as described by De Wasch and Froment [28], and Froment and Bischoff [29,30]. Bryden and Ragland [31] modelled biomass combustion in a stationary counter-flow combustor of 20 cm diameter, without considering the heat transfer by radiation in the bed. The model has been used to study the behaviour of the combustor as a function of bed length, intake air temperature, and biomass moisture and particle size.

Corella et al. [32] presented a one-dimensional steady state model of the gasification process in a fluidised bed reactor. They considered the devolatilisation of the fuel, reduction of water vapour by char and the reforming of tars. Corella and Sanz [33,34] extended the model to predict the gas composition, and tar and char contents as a function of controllable process parameters. Hamel and Krumm [35] and Oliva [36] predicted the gas composition and temperature of the different phases through all gasifier length.

A wide range of mathematical models have been presented describing the devolatilisation process. Bryden et al. [37] developed a kinetic model of biomass devolatilisation taking into account biomass drying, moisture recondensation and pyrolysis. The model is based on three parallel primary equations and two secondary equations describing the cracking of tars into char and gases. The relation between biomass particle size and the devolatilisation process has been studied by Hagge and Bryden [38]. Lapuerta et al. [39] presented a model to determine the kinetic constants of the pyrolysis process by fitting experimental thermogravimetric data (typical particle size 500 μm). The model consisted of three parallel first order reactions, which divide the process in three principal stages: biomass drying, thermal decomposition of hemicellulose and cellulose, and thermal decomposition of lignin. Porteiro et al. [40] presented a mathematical description of the thermal degradation of a densified biomass particle in an oxidising atmosphere. Thunman et al. [41] developed a dimensionless model based on the conservative equations completed with experimental data in order to predict the gas composition for any solid fuel.

Heat transfer by radiation plays an important role in the drying and devolatilisation of biomass in a co-current fixed bed gasifier. In this type of reactors, as the air and biomass flow in the same direction, the gas passes to the char reduction zone, and does not heat the incoming biomass by convection. According to Bruch et al. [19], the heat transfer by radiation is a complex phenomena, as absorption, reflection and emission of radiation are interacting. Depending upon its temperature, area and emissivity coefficient, each particle emits a certain quantity of heat to its surroundings. On the other hand, for solid fuels with a very low conductivity coefficient, as is the case for lignocellulosic biomass, the heat transfer by conduction is smaller in comparison with the heat transfer by radiation. Modest [42] described the deduction of a one-dimensional model for the radiation in a participative medium, and presented several approximate solution methodologies for this phenomenon, e.g. Schuster–Schwarzschild approximation. This model was applied by Gosman and Lockwood [43] to develop a two-dimensional model of a gas burner. Argento and Bouvard [44] determined the radiative properties of a porous medium by means of a one-dimensional steady state model. The model was used to determine the intensity of radiation within the medium in both directions (forward and backward) depending principally on the absorption and dispersion coefficients of the porous medium.

The main goal of this paper is to develop a one-dimensional steady state model for the gasification process of biomass in a fixed bed downdraft gasifier. This model, validated using experimental data obtained in a lab-scale gasifier [45], can simulate the dynamic behaviour of stratified downdraft gasifiers. The stationary approach allows an improvement in the integration precision through the all process; while the integration of the differential equations

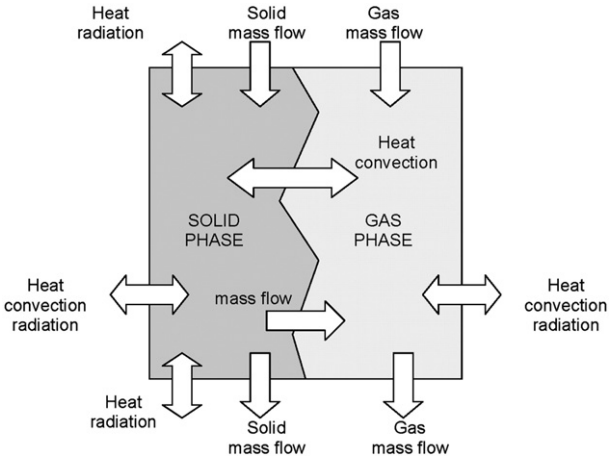

Fig. 1 – Outline of the mass and energy flows considered in the model.

under a transient approach needs more computational time. Additionally, the model considers two sub-models regarding the heat transfer through the wall, transient and steady. This is useful to simulate both kinds of experiments: the flame front moving or not through the gasifier length.

2. Mathematical model and experimental setup

The gasification process involves several phenomena. The model presented in this research paper takes into account the following:

- Moisture evaporation and biomass devolatilisation. Volatile matter content depends upon the type of biomass (proximate analysis).
- Heterogeneous reactions of the char with water vapour, carbon dioxide, hydrogen and oxygen. This kind of reactions is modelled by means of the ash segregation model (exposed core) [23,46,47].
- Combustion of the volatile matter (oxidation of carbon monoxide, hydrogen, methane and tars).
- Reforming reactions of methane and tars.
- The water gas shift reaction.
- Mass and heat transfer along the bed; heat transfer between solid-gas, solid-walls and gas-walls.
- Heat transfer by radiation in the solid phase.
- Variation of the bed void fraction though all length of the gasifier.
- Variation of the transversal section of the gasifier (geometry).
- Variation of the biomass particles diameter.
- Pressure losses in the bed.

Additionally, the following hypotheses are assumed:

- The bed is a continuous medium in steady state.
- The mean value has been used for all parameters (one-dimensional model) in the transversal section of the gasifier.
- The solid particles are assumed thermally thin (isothermal state).
- The gaseous phase is transparent to heat transfer by thermal radiation, due to its negligible absorption coefficient compared to the solid phase.
- The mass transfer by diffusion along the gasifier can be neglected compared with the mass transfer by convection.
- The properties of the gaseous phase follow the ideal gas laws.
- The ashes do not react with other species in the reactor.
- The particle geometry is considered spherical.

The most widely used parameter to describe the shape of a particle is the sphericity, which is given by the ratio of the surface area of a sphere (with same volume as the given

Table 1 – Model differential equations system

Species Conservation

–Biomass

$$d\tilde{F}_{bms}/dz = -A_s\,\tilde{r}_p \quad (1)$$

–Moisture

$$d\tilde{F}_{H2Ol}/dz = -A_s\,\tilde{r}_d \quad (2)$$

–Char

$$d\tilde{F}_{char}/dz = A_s \sum_j \nu_{char,j}\,\tilde{r}_j \quad j = p, c5, g1 - g3 \quad (3)$$

–Oxygen

$$d\tilde{F}_{O_2}/dz = -\sum_j A_i \nu_{O_2,j}\,\tilde{r}_j + \Phi_{O_2,ga} \quad j = c1 - c5 \quad i = solid, gas \quad (4)$$

–Nitrogen

$$d\tilde{F}_{N_2}/dz = \Phi_{N_2,ga} \quad (5)$$

–Steam

$$d\tilde{F}_{H_2O_v}/dz = \sum_j A_i \nu_{H_2O_v,j}\,\tilde{r}_j + \Phi_{H_2O_v,ga} \quad j = d, p, c2, c4, wg, g3 - g5 \quad (6)$$

–Carbon dioxide

$$d\tilde{F}_{CO_2}/dz = \sum_j A_i \nu_{CO_2,j}\,\tilde{r}_j \quad j = p, c3, wg, g1 \quad (7)$$

–Hydrogen

$$d\tilde{F}_{H_2}/dz = \sum_j A_i \nu_{H_2,j}\,\tilde{r}_j \quad j = p, c1, c4, wg, g2 - g5 \quad (8)$$

–Carbon monoxide

$$d\tilde{F}_{CO}/dz = \sum_j A_i \nu_{CO,j}\,\tilde{r}_j \quad j = p, c1 - c3, wg, c5, g1, g3 - g5 \quad (9)$$

–Methane

$$d\tilde{F}_{CH_4}/dz = \sum_j A_i \nu_{CH_4,j}\,\tilde{r}_j \quad j = p, c2, g2, g4 \quad (10)$$

–Tars

$$d\tilde{F}_{tars}/dz = \sum_j A_i \nu_{tars,j}\,\tilde{r}_j \quad j = p, c1, g5 \quad (11)$$

–Pressure losses

$$dP/dz = 150(1-\varepsilon)^2\varepsilon^{-3}\mu_g u_g d_p^{-2} + 1.75(1-\varepsilon)\varepsilon^{-3}\rho_g u_g^2 d_p^{-1} \quad (12)$$

–Energy conservation

–Solid phase

$$dF_{es}/dz = A(z)\cdot(dq_{rad,s}/dz) - A_s\cdot Q_{sg} - A\cdot Q_{sw} + \sum_i\sum_k A_j\cdot\nu_{i,k}\cdot\tilde{r}_k\cdot\tilde{h}_{T,i} \quad (13)$$

–Gas phase

$$dF_{eg}/dz = A_s\cdot Q_{sg} - A\cdot Q_{sw} + d/dz(A_g K_g dT_g/dz) + \sum_i\sum_k A_j\cdot\nu_{i,k}\cdot\tilde{r}_k\cdot\tilde{h}_{T,i} \quad (14)$$

–Particle diameter reduction

$$d(d_p)/dz = -(2\tilde{r}_{c5} + \tilde{r}_{g1} + \tilde{r}_{g2} + \tilde{r}_{g3})\cdot d_p/(3\cdot u_g\cdot C_{char,bms}) \quad (15)$$

Table 2 – Chemical reactions considered in the model

Process	Chemical reactions	Ref.
Drying	$R-d: H_2O_l \xrightarrow{k_d} H_2O_v$	[37]
Pyrolysis	$R-p1/R-p3: \text{biomass} = \begin{cases} \xrightarrow{k_{p1}} \text{gas} \\ \xrightarrow{k_{p2}} \text{tars} \\ \xrightarrow{k_{p3}} \text{char} \end{cases}$	[37,38,40]
Oxidation	$R-c1: C_6H_{6.2}O_{0.2} + 2.9O_2 \xrightarrow{k_{c1}} 6CO + 3.1H_2$	[16,51]
	$R-c2: CH_4 + 1.5O_2 \xrightarrow{k_{c2}} CO + 2H_2O$	[16,51]
	$R-c3: 2CO + O_2 \xrightarrow{k_{c3}} 2CO_2$	[17,52]
	$R-c4: 2H_2 + O_2 \xrightarrow{k_{c4}} 2H_2O$	[17,52]
	$R-c5: 2C + O_2 \xrightarrow{k_{c5}} 2CO$	[31]
Gasification	$R-g1: C + CO_2 \xrightarrow{k_{g1}} 2CO$	[31,46,50]
	$R-g2: C + 2H_2 \xrightarrow{k_{g2}} CH_4$	[31,46,50]
	$R-g3: C + H_2O \xrightarrow{k_{g3}} CO + H_2$	[31,46,50]
Methane reforming	$R-g4: CH_4 + H_2O \xrightarrow{k_{g4}} CO + 3H_2$	[21,22]
Tars reforming	$R-g5: C_6H_{6.2}O_{0.2} + 5.8H_2O \xrightarrow{k_{g5}} 6CO + 8.9H_2$	[32]
Water gas shift	$R-wg: CO + H_2O \xleftrightarrow{k_{wg}} CO_2 + H_2$	[33]

particle) to the particle surface area. The particle sphericity affects the heat transfer between the solid and gaseous phases. So, it is a roughly hypothesis to consider the particles as spheres. However, a wide number of models consider the biomass shape as spheres [2,13–16] due to the complexity of considering its real shape.

The gaseous phase includes the following species H_2O, H_2, CO_2, CO, CH_4, $C_6H_{6.2}O_{0.2}$ (representative for the condensable volatile matter at ambient temperature [41]), O_2 and N_2. The solid phase through all the gasifier is composed by different species such as biomass ($C_nH_mO_p$), vegetal char and ash. The moisture (H_2O_l) is inside the solid particle.

2.1. *Conservative equations*

The different mass and energy interchanges between the gaseous phase, the solid phase and the reactor wall are presented in Fig. 1. The model applies the conservative equations to a differential volume ΔV, with diameter dt and thickness Δz, along the gasifier [48]. The differential equations describing the evolution of species, energy, particle diameter and pressure losses in the bed along the reactor length are presented in Table 1. The species conservation equations are derived from the balance between the convective and source terms due to the chemical reactions developed in both phases.

The equations of energy conservation in each phase consider the heat transfer by convection between the phases and the gasifier wall, by conduction in axial direction and by radiation. The model of the absorption and emission of heat by radiation is detailed below. The energy flows related to the interchange of mass between the two phases are also taken into account.

The pressure losses along the bed are described by the equations proposed by Ergun [49], who has demonstrated that the pressure losses in a packed bed with spherical particles are caused by the loss of viscous and kinetic energy. This equation is integrated through all the length of the gasifier, considering the variation of the gas composition and assuming a linear temperature distribution in the cell.

The particle volume is considered constant during the drying and devolatilisation processes [23]. The vegetal char is assumed to be porous and the spatial structure of the particle is maintained, although its apparent density may vary. The dimensions of the particle only changes when a part of the char reacts with other species.

2.2. *Chemical reactions*

The source terms of the conservative equations are based on the reaction rates of the different chemical reactions taking place in the gasification process. In Table 2, an overview of

Table 3 – The kinetic reaction rates

Reaction	Kinetic rate [mol/m^3/s]	Ref.
R-d	$\tilde{r}_d = k_d C_{H_2O_l}$	[37]
R-p1	$\tilde{r}_{p1} = k_{p1} C_{bms}$	[37,38,40]
R-p2	$\tilde{r}_{p2} = k_{p2} C_{bms}$	[37,38,40]
R-p3	$\tilde{r}_{p3} = k_{p3} C_{bms}$	[37,38,40]
R-p	$\tilde{r}_p = C_{bms} \sum_{i=1}^{3} k_{pi}$	[37,38,40]
R-c1	$\tilde{r}_{c1} = k_{c1} T_g P^{0.3} C_{bms}^{1/2} C_{O_2}$	[16,23,51]
R-c2	$\tilde{r}_{c2} = k_{c2} T_g C_{CH_4}^{1/2} C_{O_2}$	[17,18,31]
R-c3	$\tilde{r}_{c3} = k_{c3} C_{CO} C_{O_2}^{1/4} C_{H_2O_v}^{1/2}$	[17,18,31]
R-c4	$\tilde{r}_{c4} = k_{c4} C_{H_2} C_{O_2}$	[17,18]
R-c5	$\tilde{r}_{c5} = 2\left(\frac{M_{char}}{M_{O_2}}\right) v_p \left(\frac{k_{c5} \cdot h_{m,c5}}{k_{c5} + h_{m,c5}}\right) C_{O_2}$	[31,46]
R-g1	$\tilde{r}_{g1} = \left(\frac{M_{char}}{M_{CO_2}}\right) v_p \left(\frac{k_{g1} \cdot h_{m,g1}}{k_{g1} + h_{m,g1}}\right) C_{CO_2}$	[31,46]
R-g2	$\tilde{r}_{g2} = 0.5\left(\frac{M_{char}}{M_{H_2}}\right) v_p \left(\frac{k_{g2} \cdot h_{m,g2}}{k_{g2} + h_{m,g2}}\right) C_{H_2}$	[31,46]
R-g3	$\tilde{r}_{g3} = \left(\frac{M_{char}}{M_{H_2O_v}}\right) v_p \left(\frac{k_{g3} \cdot h_{m,g3}}{k_{g3} + h_{m,g3}}\right) C_{H_2O_v}$	[31,46]
R-g4	$\tilde{r}_{g4} = k_{g4} C_{CH_4} C_{H_2O_v}$	[33]
R-g5	$\tilde{r}_{g5} = k_{g5} C_{tars}^{0.25} C_{H_2O_v}^{1.25}$	[32,33]
R-wg	$\tilde{r}_{wg} = k_{wg}\left(C_{CO} C_{H_2O_v} - \frac{C_{CO_2} C_{H_2}}{k_{wg,e}}\right)$	[17,18,23]

these chemical reactions is presented, including references of other researchers who have applied them previously. In Tables 3, 4 and 5, the kinetic reaction rates for the equations are presented. Table 6 summarises the auxiliary equations required to complete the model.

In order to characterise the composition and quantity of the pyrolyzed volatile matter of the biomass particles, the mass and energy balances for lignocellulosic biomass proposed by Thunman et al. [41,47,50] are adopted.

2.3. Auxiliary equations

To complete the source terms based on the conservation of energy, it is necessary to know the terms of heat transfer by convection between the gaseous and solid phases, and between each of these phases and the gasifier wall. The terms are calculated using the equations described by Di Blasi [17,18]. For the energy losses, the equations proposed by Hobbs et al. [1,25] have been adapted. The description of the mass and energy transfer in a packed bed by Wakao and Kaguei [59], fitting the correlations for the Nusselt and Sherwood numbers, has also been integrated in the model. Finally, the heat transfer through the gasifier walls is described by the standard equation for the heat transfer through walls, taking into account the natural convection at the reactor outside.

The temperature of each phase is obtained by an iterative process based on the integration of the mass and energy flows of each phase [9].

The passing area of the gas at a determined height of the gasifier is calculated from the bed void fraction. To determine this term, the correlation for spherical particles in a packed bed proposed by Froment and Bischoff [29,30] has been adopted.

2.4. Heat transfer by radiation

Regarding the heat transfer by radiation in the solid phase, it is assumed that this mechanism is developed through a participative medium, the fixed bed, which is constituted by the solid phase and the bed void fraction, and it is assumed that the gaseous phase is transparent to radiation. The heat transfer by radiation that travels through the bed will be attenuated by absorption and scattering effects. To model the radiation process, the approach by Schuster–Schwarzschild [15,42] has been applied. In this one-dimensional model, the direction of the heat transfer is considered perpendicular to the section of the gasifier. The medium is described as a grey and an isentropic dispersive body.

Table 4 – The kinetics constants of gas–gas reactions

k_j	A_j	Units of A_j	E_j [kJ/mol]	Ref.
k_{c1}	59.8	$kmol^{-0.5}m^{1.5}K^{-1}Pa^{-0.3}s^{-1}$	101.43	[16,23,51]
k_{c2}	9.2e6	$(m^3mol^{-1})^{-0.5}(Ks)^{-1}$	80.23	[17,18,31]
k_{c3}	$10^{17.6}$	$(m^3mol^{-1})^{-0.75}s^{-1}$	166.28	[17,18,31]
k_{c4}	1e11	$m^3mol^{-1}s^{-1}$	42	[17,18]
k_{g4}	3015	$m^3mol^{-1}s^{-1}$	125.52	[33,34,53]
k_{g5}	70	$m^3mol^{-1}s^{-1}$	16.736	[32,33]
k_{wg}	2.78	$m^3mol^{-1}s^{-1}$	12.6	[17,18,23]
$k_{wg,e}$	0.0265	–	32.90	[17,18,23]

Table 5 – The kinetics constants of solid–gas reactions

k_j	A_j	Units of A_j	E_j [kJ/mol]	Ref.
k_d	5.13e10	s^{-1}	88	[37]
k_{p1}	1.44e4	s^{-1}	88.6	[37,38,40]
k_{p2}	4.13e6	s^{-1}	112.7	[37,38,40]
k_{p3}	7.38e5	s^{-1}	106.5	[37,38,40]
k_{c5}	$1.7T_s$	$m\ s^{-1}$	74.83	[31,47,50,54]
k_{g1}	$3.42T_s$	$m\ s^{-1}$	129.7	[31,47,50,54]
k_{g2}	$1e{-}3k_{g1}$	$m\ s^{-1}$	129.7	[31,47,50,54]
k_{g3}	$1.67k_{g1}$	$m\ s^{-1}$	129.7	[31,47,50,54]

The radiation travels in both directions, and each radiative term has to be integrated separately. The intensity of radiation is attenuated by an absorption coefficient ka ($1/m$), which is a function of particle size and bed void fraction. This radiation intensity increases with the radiation emitted by the particles, and thus depends on the local temperature of the solid phase. The term corresponding to the scattering of the energy flow has been neglected ($ks=0$) [15].

2.5. Solving methodology

The ordinary differential equation system is integrated through all the gasifier length with an algorithm with variable step, which is able to reduce the length of the step interval whenever it is necessary. At the same time, this type of algorithm diminishes the computational time and improves the precision of the model.

The solution of the model is obtained by an iterative process. Based on an initial temperature profile of the solid and gaseous phases, the heat transfer by radiation is calculated allowing integrating the equations in the direction of the moving biomass and air. At the end, the temperature profile predicted by the model is compared with the initial estimated temperatures, and the model is iterated with the new temperature profile. The methodology is outlined in Fig. 2.

In the case of an entrained flow gasifier, all flows move in the same direction, except the heat transfer by thermal radiation, which initiates the drying and pyrolysis process of biomass.

Another difference with respect to the models presented in the literature is that the energy flows are integrated in each incremental step, instead of the temperature (see Eqs. (13) and (14)). As a result, the temperature of each phase is estimated by means of an iterative process using the energy balance equation of each phase.

2.6. Experimental setup

In order to obtain a simple and repetitive series of experiments, the experimental facility presented in Fig. 3 was designed and constructed [45]. The installation consists of an inverted downdraft fixed bed gasifier (50 mm diameter and 700 mm length). The air flow is controlled by a system of pressure regulators and valves and its value is estimated through the differential pressure measured over a calibrated nozzle. The gasifier is filled with biomass and it is ignited on top. Simultaneously, the air is introduced at the bottom of the gasifier. The reaction front of the gasification process goes down the gasifier until it reaches the bottom.

Table 6 – The auxiliary equations of the model

Property	Correlation/value	Ref.
Solid phase		
Specific heat [J/kg/K]	$C_{p,\mathrm{bms}} = 3.86T + 103.1$	[37,38]
	$C_{p,\mathrm{H_2O_l}} = 4180$	[37,38]
	$C_{p,\mathrm{char}} = 0.36T + 1390$	[37,38]
Thermal conductivity [W/m/K]	$K_s = 0.13 + 3e - 4(T - 273)$	
Formation enthalpy [J/mol]	$\tilde{h}^{o}_{f,\mathrm{bms}} = \mathrm{LHV_{bms}} + (1/M_{\mathrm{bms}}) \sum_{i=\mathrm{prod}} \nu_i \tilde{h}^{o}_{f,i}$	[9]
	$\tilde{h}^{o}_{f,\mathrm{char}} = 0$	[23]
	$\tilde{h}^{o}_{f,\mathrm{H_2O_l}} = -285.8e3$	[23]
Low heating value [kJ/kg]	$\mathrm{LHV_{char}} = 31,300$	[41,50]
Gas phase		
Universal gas constant [J/mol/K]	8.314	[55]
Specific heat [J/mol/K]	$C_{p,j} = A + Bt + Ct^2 + Dt^3 + E/t^2$	[56]
	$\therefore j = \mathrm{CO}, \mathrm{CO_2}, \mathrm{H_2}, \mathrm{H_2O_v}, \mathrm{CH_4}, \mathrm{N_2}, \mathrm{O_2}$ and $t = T(\mathrm{K})/1000$	
	$C_{p,\mathrm{tars}} = 88.627 + 0.12074T - 0.12735 \cdot 10^{-4}T^2 - 0.36688 \cdot 10^{7}/T^2$	[23]
Thermal conductivity [W/m/K]	$K_g = 25.77 \cdot 10^{-3}$	[57]
Formation enthalpy [kJ/mol]	$\tilde{h}^{o}_{f,j} = H$	[56]
	$\tilde{h}^{o}_{f,\mathrm{tars}} = 82.927$	[58]
Low heating value [kJ/kg]	$\mathrm{LHV_{tars}} = 40,579$	[58]
Nusselt number	$Nu = 2 + 1.1\mathrm{Re}^{0.6}\mathrm{Pr}^{1/3}$	[59]
Sherwood number	$Sh = 2 + 0.6\mathrm{Re}^{0.6}\mathrm{Sc}^{1/3}$	[59]

During the course of the experiment, the temperature profile over the entire gasifier is measured by eight thermocouples, K-type, installed with separation of 30 mm. In order to avoid interferences in the random distribution of the solid fuel inside the gasifier, and the formation of bridging (air channels), the thermocouples have been introduced only 5 mm.

From the obtained data, it is possible to calculate the biomass consumption rate. The air superficial velocity is also

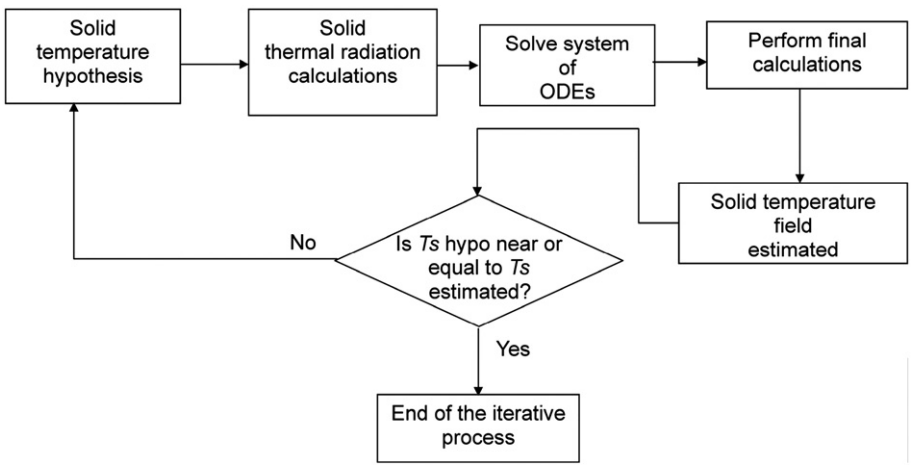

Fig. 2 – Flow chart of the model solution methodology by means of an iterative process.

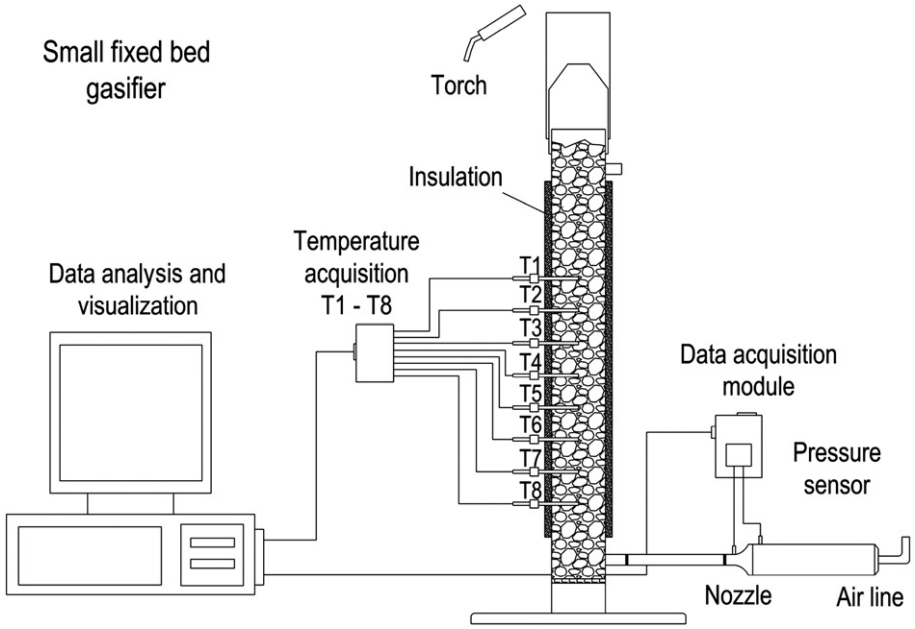

Fig. 3 – Experimental facility, inverted fixed bed downdraft gasifier.

estimated from the air flow. A typical temperature profile from the experimental setup is shown in Fig. 4. This is the initial point for the calculation of the variables. Whit the air superficial velocity, the temperature profile, the biomass composition and its density, it is possible to estimate parameters such as the fuel/air equivalence ratio, the propagation velocity of the process, maximum temperature, and others [45].

2.6.1. *Experimental design*

The experimental data used to validate the model have been published by Tinaut et al. [45]. Where was studied the effect of biomass size and air flow on biomass gasification process by means of a factorial experimental design 3^2. The experiments were carried out randomly with an air flow of 6, 12 and 18 l/min, and biomass sizes of 2–6 (4), 6–12 (9) and 12–19 (15) mm (mean diameter). All combinations between the levels of the two factors were developed in the gasification experiments, plus three replicates in the central point.

The experimental design levels and its codification are shown in Table 7. This information will be useful in the next section. The biomass tested is Pine bark with 10.9% of moisture; its ultimate and proximate analyses were done by a certified laboratory, and are shown in Table 8.

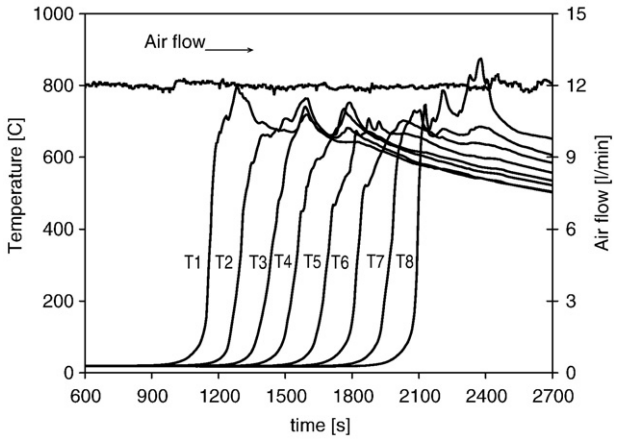

Fig. 4 – Typical temperature and supplied airflow profiles from the experimental setup.

3. Model validation

In this section the parameters calculated by the model (mod) and the experimental results obtained through the experimental design (exp) are presented. The temperature profile over the entire gasifier length, maximum process temperature, biomass burning rate, relative fuel/air ratio and process propagation velocity are contrasted for each experimental condition presented in Table 7.

3.1. *Temperature fields*

The comparison between the experimental and calculated temperature fields in the nine test points (Table 7) is presented in Fig. 5. For this study, it is necessary to convert the

Table 7 – Codification of the experimental design

dp [mm]	Superficial velocity [m/s]		
	0.05	0.1	0.15
4	C9	C2	C12
9	C10	C5	C11
15	C3	C6	C4
Air [l/min]	6	12	18

Table 8 – Ultimate and proximate analysis of Pine bark

Parameter	Ultimate analysis (%d.b.)
C	55.49
H	5.56
N	0.17
S	0.09
O[a]	37.74
Parameter	**Proximate analysis**
Volatile matter	62.521
Fixed carbon[a]	25.73
Moisture	10.91
Ash content	0.85
LHV (d.b.)	19,967.86 kJ/kg

[a] Calculated.

experimental temporary scale of the temperature profiles to the space scale in order to obtain a common basis for the comparison of different experiments. This is done by multiplying the sampling time by the flame front propagation velocity of the experiment. In each experiment the profiles of the eight signals given by the thermocouples are very similar. This is an indication that there was no air channelling during the experiments due to the thermocouple inside the bed. The experimental temperature measured during the gasification process is slightly lower than the calculated solid temperature in the nine points studied. This difference is obtained because the temperature was measured very near to the gasifier wall (5 mm deep). In this point inside the gasifier the temperature is smaller than in the central point. One of the hypotheses of the model assumes the mean value for all parameters (one-dimensional model) in the gasifier transversal section. As a result, the estimated temperature is magnified with respect to the experimental field. Nevertheless, the estimated temperatures follow the same trend as the experimental ones, which is an indicator of an appropriate heat transfer model of the biomass gasification process.

3.2. *Maximum temperature*

The maximum temperature registered experimentally and estimated by the model in the nine points tested is shown in Fig. 6. It is observed that both temperatures (solid and gas phase) are directly proportional to the air flow because the process is near to the stoichiometric fuel/air ratio (combustion). On the other hand, the biomass size does not show a clear influence on the maximum temperature. Similar results have been shown by Tinaut et al. [45] in an experimental study of the biomass gasification process.

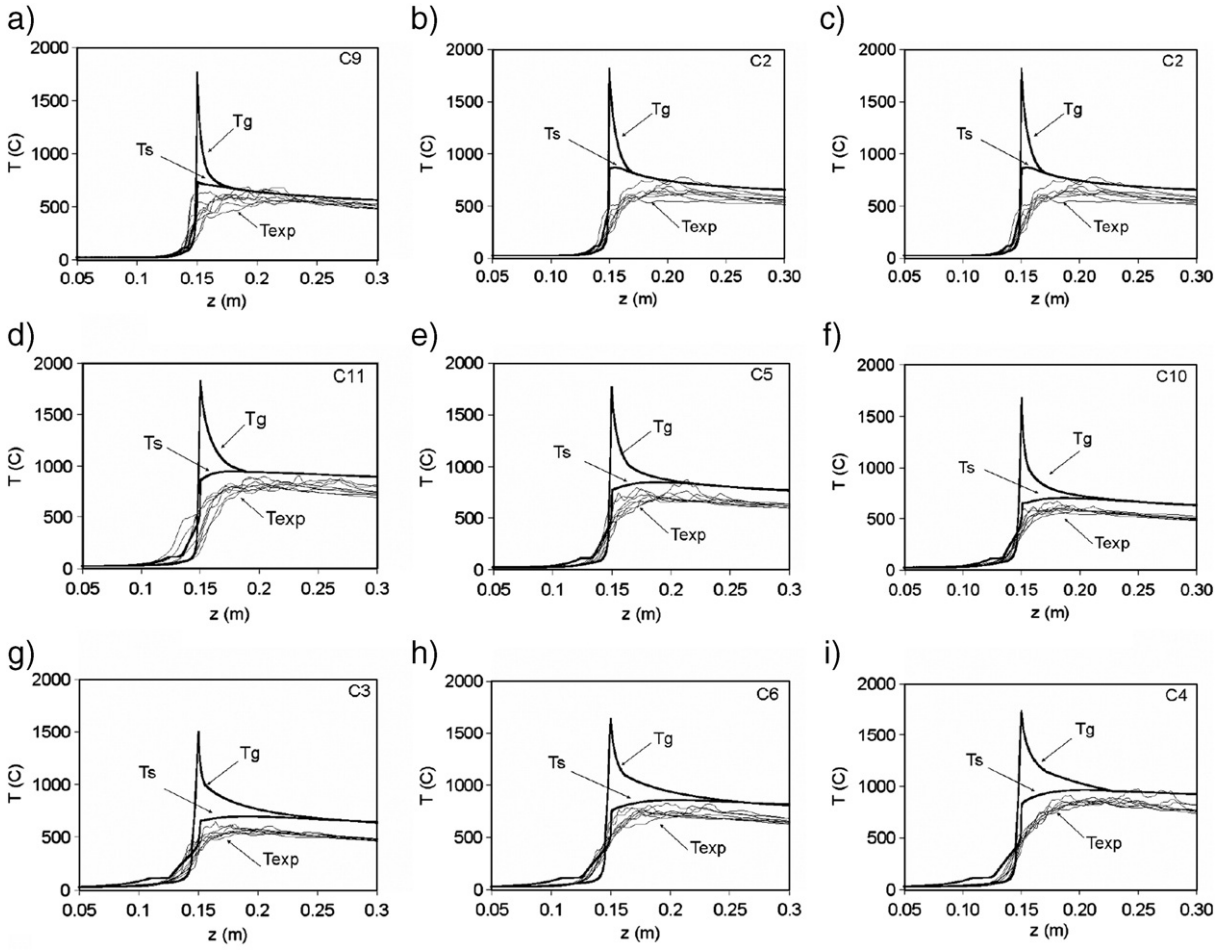

Fig. 5 – Simulated and experimental temperature profiles in the nine test points.

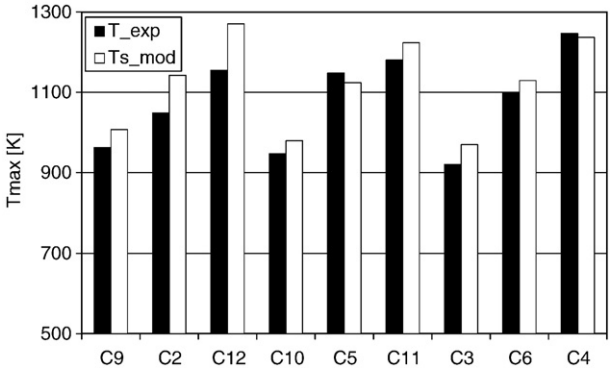

Fig. 6 – Simulated and experimental maximum temperatures for the solid phase.

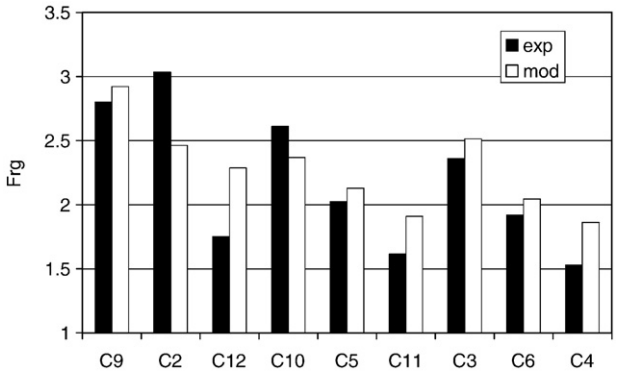

Fig. 8 – Simulated and experimental fuel/air equivalence ratio.

3.3. *Biomass consumption rate*

The biomass consumption rate per gasifier section is directly proportional to the air flow in the studied points and inversely proportional to the size of biomass, due to the increasing reaction area with reduced particle size. In Fig. 7a the validation of this parameter with the experimental results is presented. A good agreement between the experimental measurements and model simulations can be observed. A similar trend is shown for the process propagation velocity (Fig. 7b).

For low diameters the model underestimates the experimental results, regarding with the biomass consumption rate and the process propagation velocity. Although the heat transfer between solid and gaseous phases is higher when biomass size diminishes, the heat transfer by radiation penetration is reduced (this mechanism drives the drying and devolatilization process), thereby the biomass consumption rate and the flame front velocity is underestimated. Furthermore, the solid/gas heat transfer coefficient estimated from nonreacting systems can exceed the experimental values in reacting gasifiers. Therefore, the experimental correlation is multiplied by empirical factors with values in the range 0.02–1 [17]. Due to the wide range of variation of the empirical factor, it is possible that the model does not simulate adequately all experimental points.

3.4. *Gasification relative fuel/air ratio*

The gasification relative fuel/air ratio is inversely proportional to the air flow and to biomass size. If the amount of air increases, the thermochemical process approximates to the combustion. On the other hand, the increasing particle size results in diminished density as the amount of biomass per volume decreases. This parameter is presented in Fig. 8. The trend exhibited by the model is very similar to the experimental results. Nevertheless, in some points, this variable is slightly overestimated by the model due to the overestimation of the reaction temperature, which in turn leads to a slightly higher reaction rate (experiment C12). On the other hand, the underestimation of the gasification relative fuel/air ratio in the C2 point, is related with the underestimation of the biomass consumption rate (Fig. 7a), described in the Section 3.3, due to the direct relationship between the biomass consumption and relative fuel/air ratio.

4. Other results of the model

4.1. *Temperature field*

Characteristics such as solid and gas species evolution, particle diameter, solid and gas velocities, the different stages

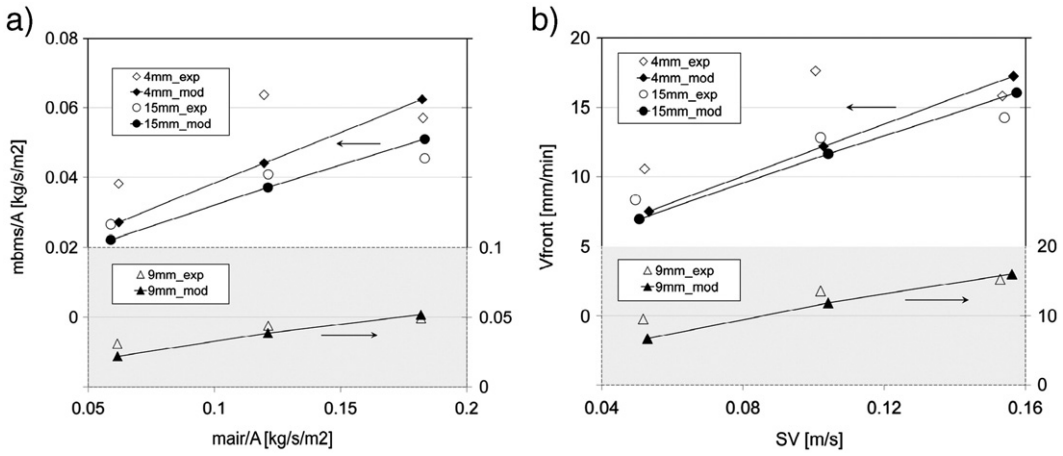

Fig. 7 – Effect of the air supply rate and the biomass size on the biomass burning rate (a) and the process propagation velocity (b).

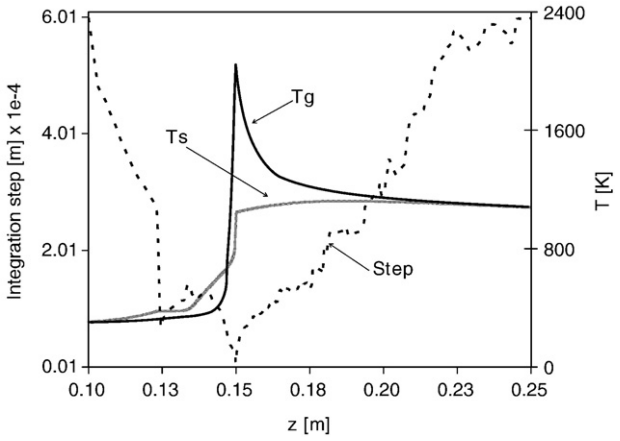

Fig. 9 – Simulated temperature profile over the entire length of the gasifier and the integration step with SV = 0.1 m/s and biomass size of 6–12 mm (C5 conditions).

of the gasification process and the heat transfer mechanisms in the bed, which are rather hard to measure by conventional techniques, are presented in this section. Next, the results are presented for the central experimental point (conditions C5 in Table 7).

The evolution of solid and gas temperatures through the gasifier length are shown in Fig. 9. It can be observed how the heating starts in the solid phase due to the radiative heat transfer from the stages at high temperature in the combustion/oxidation zone. The gaseous species are heated by convection between the solid and gas phases. During the subsequent drying process the temperature of the solid phase is stabilized. Once this drying process has finished, the temperature increases until pyrolysis temperatures are reached. At a specific time, the gas phase temperature increases suddenly because the combustion of volatiles with oxygen has initiated. This effect is accompanied by the oxidation of char, and thereby, also the solid temperature is increased. Once the oxygen has been consumed by the oxidation reactions, the gas temperature does not increase and the reduction reactions propagate mainly by the thermal energy available in the gas phase. At the same time the gas phase transfers a part of its energy to the solid until the thermal equilibrium is reached, in this stage the chemical reactions are frozen, and the solid and gas temperatures diminish, mainly due to the heat losses at the gasifier wall.

As the char is consumed during the reduction reactions, the heat transfer area between the solid and gas phase increases. This change in the particle surface area causes that both temperatures get equal faster. In the same Figure, the average integration step is showed, which is modified in function of the mathematical precision of the model. It can be seen that the integration step is minimal in the reaction stages.

4.2. *Solid and gas species evolution*

The evolution of the solid phase species, the oxygen content of the gaseous phase and the solid and gas temperatures are shown in Fig. 10a. It can be observed that the first process is the biomass drying. In a second step, the solid temperature begins to increase until biomass is pyrolyzed. Subsequently combustion is initiated at the same time that pyrolysis is in course; this process is denominated flaming-pyrolysis stage by Di Blasi [17].

Volatiles and pyrolyzed char react with oxygen. The combustion of volatiles increases the gas temperature, which in turn heats the solid. Once the oxygen is consumed, the pyrolysis can continue if not all the biomass has been consumed. On the other hand, the high amount of thermal energy in the process allows the reduction reactions to begin.

Fig. 10b shows the results from the reduction stage. During this stage, the CO and H_2 are generated by reforming of the tars with steam. At the same time, the CO_2 is reduced with char to produce CO. At the end of the reduction stage, when the temperature falls below specific levels, all chemical reactions are frozen, except the water–gas shift reaction, which slightly favours the formation of H_2 instead of CO.

4.3. *Particle diameter and pressure losses*

The evolution of the particle diameter and the pressure losses of the gas phase are shown in Fig. 11a. It can be seen that the diameter begins to diminish just at the moment when

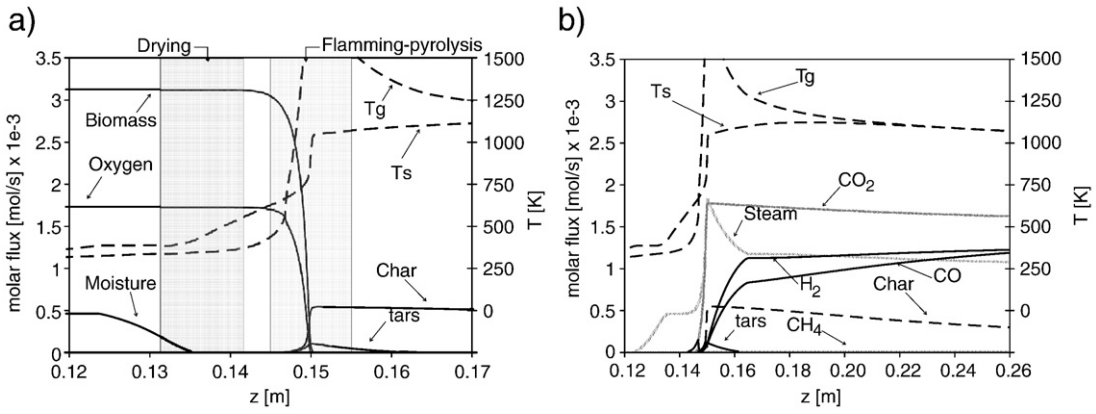

Fig. 10 – The different identified stages and evolution of the species over the entire length of the gasifier (C5 conditions). a) Drying and flaming-pyrolysis stages; b) Reduction stage.

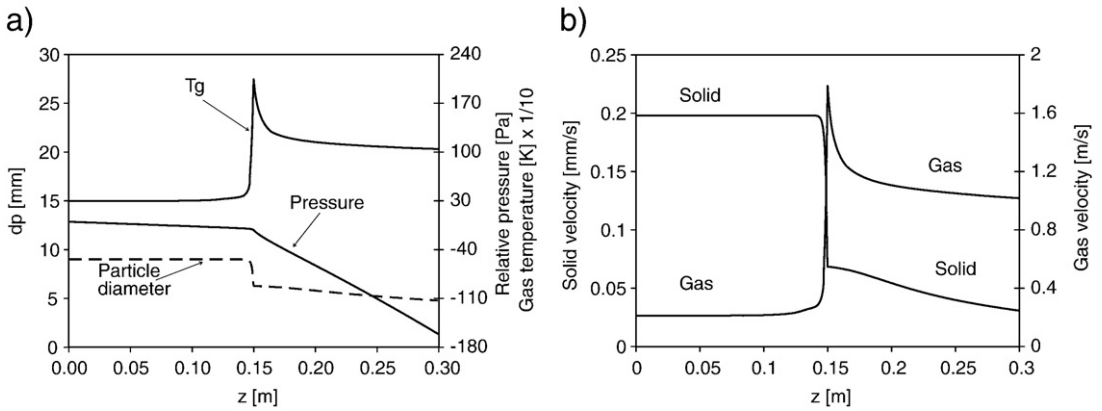

Fig. 11 – The evolution of the particulate diameter and pressure losses (a) and the solid and gas phase velocity (b) over the entire length of the gasifier (C5 conditions).

combustion starts. The char is thus also oxidized and causes the reduction in diameter. During the reduction stage, the diameter diminishes more slowly as the char gasification takes place.

The pressure losses at the top of the gasifier diminish slowly, but after the oxidation stage, this parameter changes drastically due to the reduction of the particle diameter and to the higher temperature and mass of the gas phase.

4.4. *Solid and gas velocities*

The evolution of the solid and gas velocities over the entire length of the gasifier are shown in Fig. 11b. In the first part, both velocities remain constant. In the reaction stage, the velocity of the gas increases due to the increase of the mass and temperature of this phase. On the other hand, the solid velocity diminishes due to the reduction of the particle diameter and the consumption of the solid species. It is also shown that when the temperature of the gas phase diminishes, its velocity also decreases.

4.5. *Heat transfer mechanisms in the bed*

In order to discuss the relation between the most important processes and the velocity of the reaction front, the solid and gas temperature field, and the evolution of the different heat transfer mechanisms considered in the model are presented in Fig. 12.

In the drying and pyrolysis stages, the energy is mainly transmitted by radiative heat transfer. Within the same stages, the heat transfer between the solid and gas phase is very important. In the simulated process, the solid heats the gas phase in the pyrolysis area because at this point, the solid is hotter due to the high amount of absorbed radiation. The gas warms up until the combustion reactions are initiated. When an important increase in gas temperature occurs due to the combustion of volatiles, the heat transfer between solid and gas is inverted, and the gas further heats the solid phase. The temperature of the solid increases very fast and is directly proportional to the gas temperature. The point of maximum solid temperature is given by the thermal equilibrium between the heat losses by radiation and the heat transmitted by the gas phase.

From this point, the solid temperature does not change significantly. It even can increase slightly until the equilibrium with the temperature of gaseous phase is reached. Thereby, the radiation losses diminish although the temperature also diminishes due to the energy consumption by the chemical reduction reactions and the heat loss through the wall of the gasifier. It has to be highlighted that the heat transfer by conduction in the gas phase is not as important as the other considered energy transport phenomena.

In Fig. 13, the main energy flows are outlined. Their interaction and their effect on the evolution of the biomass gasification process in a downdraft fixed bed gasifier are indicated. The radiative heat transfer in the solid phase initiates the pyrolization of the biomass. Subsequently the producer gas–air mixture is heated by the heat transfer from the solid to the gas phase until combustion is started. At that moment the gas phase heats the solid and this mechanism allows the existence of radiative heat transfer to the wet biomass

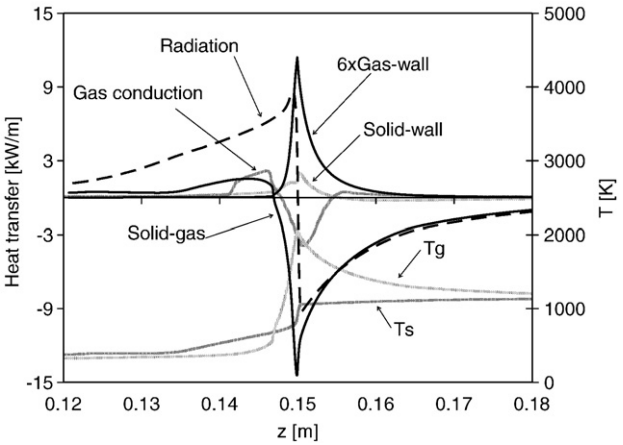

Fig. 12 – Evolution of the heat transfer by convection, conduction and radiation in the main stage of the gasification process (C5 conditions).

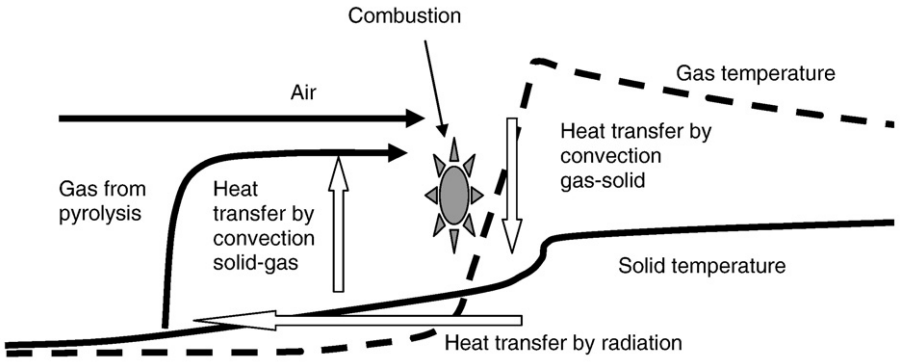

Fig. 13 – Interaction mechanism of the main energy flows in the reaction front.

approximating to the reaction front, which leads to a sustainable auto thermal mechanism for the gasification process.

5. Conclusions

A steady, one-dimensional model of the biomass gasification process has been developed. The model considers the main processes that are relevant for the thermochemical transformation of biomass in a gaseous fuel that can be used in reciprocating internal combustion engines.

The model has been validated with biomass of different size and varying the air superficial velocity. A reasonable agreement between the experimental and calculated results has been achieved. The developed model thus simulates satisfactorily the main sub-processes of the biomass gasification process.

The gasification model allows evaluating the effect of the physical, chemical and energy properties of biomass (size, density, proximate and ultimate analysis, and heating value) on the gasification process. Moreover, it enables the study of the gasifier geometry, the heat exchange and the different injection points of the gasifying agent.

The producer gas composition calculated by the model can be used to predict the performance and pollutant emissions of an engine that is fuelled with the gas.

The main energy fluxes in the gasification process have been analyzed by the model, and the most important flux is the heat transfer by radiation in the solid phase, which facilitates the drying and devolatilization processes, thus opening the way to the combustion stage.

The model can be used as a design tool for downdraft gasifiers; it gives the thermal power generated, the flow and the composition of the producer gas, the global efficiency of the process, and others.

The different stages of the gasification process and the heat transfer mechanisms in the bed (hard to measure by conventional techniques) have been recognized and analysed, and it is proposed a possible sustainable auto thermal mechanism of the flame front in downdraft fixed bed gasifiers.

Nomenclature

A	Gasifier area (m^2)
A_j	Phase j area (m^2)
A_j	Pre-exponential factor
$C_{char,bms}$	Initial mol char per biomass mol (mol/m^3)
$C_{p,i}$	Specific heat of the species i (kJ/kg/K or J/mol/K)
D_j	Diffusion coefficient (m^2/s)
dp	Particle diameter (m)
dt	Reactor diameter (m)
E_j	Activation energy of the reaction j (kJ/mol)
$F_{e,i}$	Energy flow of the species i (J/s)
$\tilde{F}_i$	Molar flow of the species i (mol/s)
F_{rg}	Fuel/air equivalence ratio (–)
H	Convection heat transfer coefficient ($W/m^2/K$)
$\tilde{h}^{o}_{f,i}$	Formation enthalpy of species i (J/mol)
$h_{m,j}$	Mass transfer coefficient of the reaction j (m/s)
$\tilde{h}_{T,i}$	Total enthalpy of species i (J/mol)
I_d, I_i	Radiation intensity (W/m^2)
I_b	Black body radiation intensity (W/m^2)
k_a	Absorption coefficient (m^{-1})
k_j	Thermal conductivity of the phase j (W/m/K)
k_j	Kinetic constant of the reaction j
m_{air}	Mass flow rate of air (kg/s)
m_{bms}	Mass flow rate of biomass (kg/s)
M_i	Molecular weight of the species i (kg/kmol)
P	Pressure (Pa)
Q	Volumetric heat transfer by convection (W/m^3)
q_{rad}	Radiation heat transfer in the solid phase (W/m^2)
$\tilde{r}_j$	Kinetic reaction rate ($mol/m^3/s$)
SV	Air superficial velocity (m/s)
T	Temperature (K)
t	Time (s)
u_j	Velocity of phase j (m/s)
V_{front}	Process propagation velocity (mm/min)
V_p	Solid particle volume (m^3)
$Y_{char,bms}$	Initial char molar fraction per biomass mol
Z	Integration axial coordinate (m)

Greek letters

ε	Bed void fraction
ε'	Radiation emissivity
μ_g	Gas viscosity (kg/m/s)
$\nu_{i,j}$	Stoichiometric coefficient of species i in reaction j
ν_p	Particle density number (m^{-1})
$\Phi_{i,ag}$	Gasifying agent source term for species i (mol/m/s)
ρ_j	Mass concentration (kg/m^3)
σ_s	Scattering coefficient (m^{-1})
σ	Stefan–Boltzmann constant 5.76×10^{-8} ($W/m^2/K$)

Subscripts

ag	Gasifying agent
exp	Experimental
g	Gas
g,w	Gas/wall
gs	Gas/solid
rad, *s*	Radiation in the solid phase
s	Solid
s,w	Solid/wall
sg	Solid/gas
w	wall

Acknowledgements

The authors would like to thank the Spanish Ministry of Education and Science for the financial support of this research through project REN2003-09299/TECNO and the Programme AlBan, The European Union Programme of High Level Scholarship for Latin America, scholarship no. E04D046253CO. Help from Dr. Hannes Laget (Laborelec, Belgium) is also gratefully acknowledged.

REFERENCES

[1] M.L. Hobbs, P.T. Radulovic, L.D. Smoot, Combustion and gasification of coals in fixed-beds, Progress in Energy and Combustion Science 19 (1993) 505–586.
[2] Y. Yang, V. Sharifi, J. Swithenbank, Effect of air flow rate and fuel moisture on the burning behaviours of biomass and simulated municipal solid wastes in packed beds, Fuel 83 (2004) 1553–1562.
[3] M. Ruggiero, G. Manfrida, An equilibrium model for biomass gasification processes, Renewable Energy 16 (1999) 1106–1109.
[4] C. Altafini, P. Wander, R. Barreto, Prediction of the working parameters of a wood waste gasifier through an equilibrium model, Energy Conversion and Management 44 (2003) 2763–2777.
[5] Altafini, A. Mirandola, A chemical equilibrium model of the coal gasification process based on the minimization of the Gibbs free energy, Florence World Energy Research Symposium-FLOWERS97, Florence, Italy, 1997.
[6] M. Lapuerta, J.J. Henández, F.V. Tinaut, A. Horrillo, Thermochemical behaviour of producer gas from gasification of lignocellulosic biomass in SI engines, SAE Paper (2001) Series 2001-01-3586.
[7] M. Lapuerta, A. Horrillo, J.J. Hernández, A. Diez, Simulation of producer gas utilization from gasification of lignocellulosic biomass wastes in reciprocating internal combustion engines: effects on performances and pollutant emissions, in: S. Kyritsis, A.A.C.M. Beenackers, P. Helm, A. Grassi, D. Chiaramonti (Eds.), First World Conference on Biomass for Energy and Industry, Proceedings of the Conference held in Sevilla, Spain, 5–9, June 2000, James and James (Science Publishers) Ltd, London, 2001, pp. 1929–1932.
[8] X. Li, J.R. Grace, A.P. Watkinson, C.J. Lim, A. Ergudenler, Equilibrium modeling of gasification: a free energy minimization approach and its application to a circulating fluidized bed coal gasifier, Fuel 80 (2001) 195–207.
[9] A. Melgar, J.F. Pérez, H. Laget, A. Horrillo, Thermochemical equilibrium modelling of a gasifying process, Energy Conversion and Management 48 (2007) 59–67.
[10] M. Rashidi, Calculation of equilibrium composition in combustion products, Applied Thermal Engineering 18 (1998) 103–109.
[11] G. Schuster, K. Loffler, H. Weigl, Biomass steam gasification an extensive parametric modeling study, Bioresource Technology 77 (2001) 71–79.
[12] Z. Zainal, R. Ali, C. Lean, K. Seetharamu, Prediction of performance of a downdraft gasifier using equilibrium modeling for different biomass materials, Energy Conversion and Management 42 (2001) 1499–1515.
[13] Y. Yang, V. Sharifi, J. Swithenbank, Converting moving-grate incineration from combustion to gasification. Numerical simulation of the burning characteristics, Waste Management 27 (2006) 645–655.
[14] Y. Yang, V. Sharifi, J. Swithenbank, Substoichiometric conversion of biomass and solid wastes to energy in packed beds, AIChE Journal 52 (2006) 809–817.
[15] D. Shin, S. Choi, The combustion of simulated waste particles in a fixed bed, Combustion and Flame 121 (2000) 167–180.
[16] Y. Yang, H. Yamauchi, V. Nasserzadeh, J. Swithenbank, Effects of fuel devolatilisation on the combustion of wood chips and incineration of simulated municipal solid wastes in a packed bed, Fuel 82 (2003) 2205–2221.
[17] C. Di Blasi, Dynamic behaviour of stratified downdraft gasifiers, Chemical Engineering Science 55 (2000) 2931–2944.
[18] C. Di Blasi, Modeling wood gasification in a countercurrent fixed-bed reactor, AIChE Journal 50 (2004) 2306–2319.
[19] C. Bruch, B. Peters, T. Nussbaumer, Modelling wood combustion under fixed bed conditions, Fuel 82 (2003) 729–738.
[20] T. Jayah, L. Aye, R. Fuller, D.F. Stewart, Computer simulation of a downdraft wood gasifier for tea drying, Biomass and Bioenergy 25 (2003) 459–469.
[21] D.L. Giltrap, R. McKibbin, G. Barnes, A steady state model of gas-char reactions in a downdraft biomass gasifier, Solar Energy 74 (2003) 85–91.
[22] B.V. Babu, P. Sheth, Modeling and simulation of reduction zone of downdraft biomass gasifier: effect of char reactivity factor, Energy Conversion and Management 47 (2005) 2602–2611.
[23] M. De Souza-Santos, Solid Fuels Combustion and Gasification. Modeling, simulation and equipment operation, Marcel Decker Inc., New York, 2004.
[24] M. Hobbs, P. Radulovic, L.D. Smoot, Chemical and physical processes in countercurrent fixed-bed coal gasification, 23rd Symposium of the Combustion Institute, 1990.
[25] M.L. Hobbs, P.T. Radulovic, L.D. Smoot, Modeling fixed-bed coal gasifiers, AIChE Journal 38 (1992) 681–702.
[26] M.U. Ghani, P.T. Radulovic, L.D. Smoot, An improved model for fixed-bed coal combustion and gasification: sensitivity analysis and applications, Fuel 75 (1996) 1213–1226.
[27] P. Radulovic, M. Ghani, L.D. Smooth, An improved model for fixed bed coal combustion and gasification, Fuel 74 (1995) 582–594.
[28] A.P. DeWasch, G.F. Froment, Heat transfer in packed beds, Chemical Engineering Science 27 (1972) 567–576.
[29] G. Froment, K. Bischoff, Chemical Reactor Analysis and Design, first ed.John Wiley and Sons, New York, 1979.
[30] G. Froment, K. Bischoff, Chemical Reactor Analysis and Design, second ed.John Wiley and Sons, New York, 1990.
[31] K.M. Bryden, K. Ragland, Numerical modeling of a deep, fixed bed combustor, Energy & Fuels 10 (1996) 269–275.
[32] J. Corella, J.M. Herguido, J. Toledo, I. Gómez, Modelling fluidized bed gasifiers. Part II: gasification with steam in a bubbling fluidized bed, 1st World Conference on Biomass for Energy and Industry, vol. II, Sevilla, Spain, 2000.
[33] J. Corella, A. Sanz, Modeling circulating fluidized bed biomass gasifiers. A pseudo-rigorous model for stationary state, Fuel Processing Technology 86 (2005) 1021–1053.
[34] C. Sanz, J. Corella, Modeling circulating fluidized bed biomass gasifiers. Results from a pseudo rigorous 1 dimensional model for stationary state, Fuel Processing Technology 87 (2006) 247–258.

[35] S. Hamel, W. Krumm, Mathematical modelling and simulation of bubbling fluidised bed gasifiers, Powder Technology 120 (2001) 105–112.
[36] D. Oliva, Combustión del bagazo de caña de azúcar en lecho fluidizado (in Spanish). PhD Thesis, Universidad de Valladolid, 1999.
[37] K.M. Bryden, K. Ragland, C. Rutland, Modeling thermally thick pyrolysis of wood, Biomass and Bioenergy 22 (2002) 41–53.
[38] M. Hagge, K.M. Bryden, Modeling the impact of shrinkage on the pyrolysis of dry biomass, Chemical Engineering Science 57 (2002) 2811–2823.
[39] M. Lapuerta, J.J. Hernández, J. Rodríguez, Kinetics of devolatilization of forestry wastes from thermogravimetric analysis, Biomass and Bioenergy 27 (2004) 385–391.
[40] J. Porteiro, J.L. Míguez, E. Granada, J.C. Moran, Mathematical modelling of the combustion of a single wood particle, Fuel Processing Technology 87 (2006) 169–175.
[41] H. Thunman, F. Niklasson, F. Johnsson, B. Leckner, Composition of volatile gases and thermo chemical properties of wood for modeling of fixed or fluidized beds, Energy and Fuels 15 (2001) 1488–1497.
[42] M.F. Modest, Radiative Heat Transfer, second ed.Academic Press, New York, 2003.
[43] A.D. Gosman, F.C. Lockwood, Incorporation of a flux model for radiation into a finite-difference procedure for furnace calculations, 14th International Symposium on Combustion, The Combustion Institute, Pittsburgh, USA, 1972.
[44] C. Argento, D. Bouvard, A ray tracing method for evaluating the radiative heat transfer in porous media, International Journal of Heat and Mass Transfer 39 (1996) 3175–3180.
[45] F.V. Tinaut, A. Melgar, J.F. Pérez, A. Diez, Analysis of parameters influencing biomass gasification by means of a small scale fixed bed gasifier, 14th European Biomass Conference & Exhibition. Biomass for Energy, Industry and Climate. Proceedings of the Conference held in Paris, France, 17–21, October 2005.
[46] G. Borman, K. Ragland, Combustion Engineering, MacGraw-Hill, Boston, 1998.
[47] H. Thunman, Principles and models of solid fuel combustion. PhD thesis, Chalmers University of technology, 2001.
[48] R.B. Bird, S. Stewart, E: Lightfoot, Transport Phenomena, John Wiley and Sons, New York, 2002.
[49] S. Ergun, Fluid flow through packed columns, Chemical Engineering Progress 48 (1952) 89–94.
[50] H. Thunman, Combustion of Biomass — Lecture Notes of Nordic Course, Chalmers University of Technology, Sweden, 2002, www.entek.chalmers.se/~heth/nordic_course.pdf.
[51] L. Pettersson, R. Westerholm, State of the art of multi-fuel reformers for fuel cell vehicles: Problem identification and research needs, International Journal of Hydrogen Energy 26 (2001) 243–264.
[52] A. Corti, L. Lombardi, Biomass integrated gasification combined cycle with reduced CO_2 emissions: performance analysis and life cycle assessment (lca), Energy 29 (2004) 2109–2124.
[53] H. Liu, B. Gibbs, Modeling NH_3 and HCN emissions from biomass circulating fluidized bed gasifiers, Fuel 82 (2003) 1591–1604.
[54] H. Thunman, B. Leckner, F. Niklasson, F. Johnsson, Combustion of wood particles a particle model for Eulerian calculations, Combustion and Flame 129 (2002) 30–46.
[55] K. Wark, D. Richards, Termodinámica, McGraw-Hill, Madird, 2000.
[56] M.W. Chase, M.W. NIST-JANAF Thermochemical Tables. Journal physical chemical reference data, Monograph 9, New York, 1998.
[57] L.A. Nieto, Producer gas properties analysis to design a detector of the gas quality, Internal Investigation Report, Universidad de Valladolid, 2006, (in Spanish).
[58] S.R. Turns, An introduction to combustion. concepts and applications, McGraw-Hill, Inc., Singapore, 1996.
[59] N. Wakao, S. Kaguei, Heat and mass transfer in packed beds, Gordon and Breach Science, New York, 1982.